Preparation and characterization of novel lithium magnesium phosphate bioceramic scaffolds facilitating bone generation

Fupo He[a,*,1], Xinyuan Yuan[b,1], Teliang Lu[b,1], Yao Wang[a], Songheng Feng[a], Xuetao Shi[b], Lin Wang[b,*], Jiandong Ye[b], Hui Yang[c]

[a]School of Electromechanical Engineering, Guangdong University of Technology, Guangzhou 510006, People's Republic of China

[b]School of Materials Science and Engineering, South China University of Technology, Guangzhou 510641, People's Republic of China

[c]Key Laboratory of Prevention and Treatment of Cardiovascular and Cerebrovascular Diseases, Ministry of Education; School of Medical Information Engineering, Gannan Medical University, Ganzhou 341000, People's Republic of China

[1] Equal contribution to this paper

[*]Correspondence to: fphe@gdut.edu.cn (F. He); wanglin3@scut.edu.cn (L. Wang)

2. Materials and methods

2.1. Synthesis of LMP materials

Li_2CO_3, $NH_4H_2PO_4$ and $4MgCO_3 \cdot Mg(OH)_2 \cdot 5H_2O$ were used as raw materials to synthesize LMP materials and tri-magnesium phosphate (control group) by the solid-state reaction method. Three groups of LMP materials with different Li/Mg molar ratios were synthesized, including $Li_{0.5}Mg_{2.75}(PO_4)_2$, $Li_1Mg_{2.5}(PO_4)_2$, $Li_2Mg_2(PO_4)_2$. Table 1 gives the formulas and abbreviations of LMP materials and tri-magnesium

phosphate. The raw materials were weighed out based on the stoichiometric ratio, and mixed manually, then heated at 60 °C for 12 h to remove the NH_3 by decomposing $NH_4H_2PO_4$. The mixtures were mixed with anhydrous ethanol, and underwent the ball milling in a planetary ball mill (rotation rate: 300 rpm; milling time: 4 h). The obtained powder mixtures were dried in the oven, and then sieved through a 100-mesh sieve. The solid-state reaction of powder mixtures was achieved by calcination at 1000 °C for 2 h. The reaction products were ground, and screened through a 200-mesh sieve, and finally the LMP powders were obtained.

2.2. Fabrication of LMP bioceramic blocks and scaffolds

To investigate the effect of Li/Mg ratio on the densification process of LMP bioceramics, non-macroporous bioceramic blocks were prepared by compression molding. The synthesized powders (Mg3, Li0.5Mg2.75, Li1Mg2.5 and Li2Mg2) were poured into a customized mold, then pressurized under an axial compressive force of 10 MPa. The obtained compacted blocks were subjected to an isostatic pressure of 200 MPa for 2 min. The green bodies were sintered at 1050 °C for 2 h, and finally the bioceramic blocks were obtained.

Macroporous LMP bioceramic scaffolds were fabricated by an extrusion-based 3D printing equipment (3D Bio-Architectwork station, Hangzhou, China). Briefly, 8 g polyvinyl alcohol solution (8 wt%) was mixed with 10 g LMP powders and 0.3 g methylcellulose, and ground in the planetary ball mill for 2 h. The predesigned cylindrical model was loaded into the printing equipment. The prepared paste was placed in the injection cartridge of 3D printer, and then the extruded fibers stacked

layer by layer, and aligned orthogonally to form interconnected square-shaped macropores. The printed constructs were dried at 50 °C for 12 h, and then sintered at 1050 °C for 2 h. The macroporous LMP bioceramic scaffolds were acquired.

2.3. Material characterizations

Phase composition of LMP bioceramics was detected by X-ray diffraction (XRD) utilizing an X-ray diffractometer (X'Pert PRO, PANalytical Co., Netherlands) using Cu-Kα radiation at 40 kV voltage. The data acquisition range was 10-70° for 2θ, and the scanning step size was 0.01313°. Surface morphology and microstructure of LMP bioceramic blocks and scaffolds were observed using field emission scanning electron microscopy (SEM; MERLIN, Zeiss, Germany). Prior to observation, the samples mounted on the aluminum plate were sputter-coated with gold. An acceleration voltage of 10 kV was used. Differential scanning calorimetry (DSC; DSC 214 Polyma, Netzsch, Germany) was utilized to identify the melting temperature of LMP materials.

Porosity of non-macroporous LMP bioceramic blocks was tested by the Archimedes method, and the detailed test procedures are described in previous work [30]. The porosity of the macroporous LMP bioceramic scaffolds was estimated utilizing the protocols described in previous work [31]. The scaffold porosity was estimated utilizing the equation: Porosity = $(1 - \rho_1/\rho_0) \times 100\%$. ρ_1 means the density of bioceramic scaffolds, and it was determined by calculating the weight to volume ratio of scaffolds. ρ_0 represents the theoretical density of completely dense LMP bioceramics, which was determined by the pycnometric method.

A universal material testing machine was used to measure the compressive

strength of non-macroporous blocks (5 mm × 5 mm × 10 mm) and macroporous scaffolds (Φ 5 mm × 10 mm) of LMP bioceramics. A crosshead speed of 0.5 mm·min^{-1} was utilized.

2.4. Assessments of cell-biological performances

Mouse bone mesenchymal stem cells (mBMSCs; ATCC, USA) were used to assess cytocompatibility and osteogenic differentiation. Human umbilical vein endothelial cells (HUVECs; ATCC, USA) were utilized to evaluate the proangiogenic activity. mBMSCs were cultured with Dulbecco modified high glucose eagle culture medium (H-DMEM; Gibco, USA) containing 10 vol% fetal bovine serum (FBS; Gibco, USA). HUVECs were cultured in the endothelial basal medium (Lonza, Switzerland) that was added with 1% FBS and several cytokines (Lonza, Switzerland). To unveil the synergistic effects of released Li and Mg on the cell response, the cells were cultivated in the bioceramic extracts, which were fabricated according to the protocols from ISO 10993–12. Briefly, the bioceramic scaffolds were pulverized, immersed in the H-DMEM or endothelial basal medium at 37 °C for 24 h, and the ratio of scaffold weight to medium volume was 0.2 g mL^{-1}. After 24 h, the mixtures were centrifuged to collect the supernatant. For sterilization, the collected extracts were filtrated through 220 nm filtering membranes. The concentrations of Mg, Li and P in the extracts were tested by inductively coupled plasma mass spectrometry (Optimal 5300DV, Perkin Elmer, USA). The cells were seeded at a density of 2 × 10^3 cells/well. After culturing for 24 h, the complete medium was replaced by the bioceramic extracts. The extract was replaced by new one every other day. All the

biochemical kits were used following the protocols from manufacturers.

mBMSCs and HUVECs were stained using a Live/Dead kit (calcein-AM, Biotium, USA), and the cell viability was assessed by fluorescence microscopy (Axioskop 40, Zeiss, Germany). CCK-8 kit (Dojindo Laboratories, Japan) was used to detect the proliferative capacity of mBMSCs and HUVECs. As for assessments of osteogenic differentiation, alkaline phosphatase (ALP) activity of mBMSCs was determined by the p-nitrophenyl phosphate assay (p-NPP, Sigma Aldrich). ALP staining of mBMSCs was performed using an Alkaline Phosphatase Stain assay kit (Beyotime, China).

Real-time polymerase chain reaction (RT-PCR) was used to quantitatively detect the expression of genes related to osteogenic differentiation of mBMSCs and proangiogenic activity of HUVECs. After culturing for scheduled time, total RNAs of mBMSCs or HUVECs were extracted utilizing a HiPure Total RNA Micro Kit (Magen, China). The total RNAs were quantified with a Nano-drop 2000 (Thermo Scientific, USA). First strand complementary DNA was acquired from RNA by a Transcriptor First Strand cDNA Synthesis Kit (Roche, Germany). PCR assay for determining the expressions of osteogenesis– and proangiogenic-activity-related genes was conducted employing an Applied Biosystems™ QuantStudio™ 6 Flex (Thermo Fisher Scientific, USA). The osteogenesis–related genes included collagen type I (Col I), ALP, bone sialoprotein (BSP) and osteocalcin (OCN). The proangiogenic-activity-related genes included vascular endothelial growth factor (VEGF), vascular endothelial growth factor receptor 2 (KDR) and hypoxia inducible

factor-1α (HIF-1α). The primer sequences for genes are provided in the Table S1. The RT-PCR reaction was conducted in accordance with the following thermal profile: 95 °C for 30 s, followed by 95 °C for 5 s, 60 °C for 30 s with 40 cycles. The relative amount of target genes was determined by the use of a ΔCt method (ΔCt = Ct (target gene) – Ct (GAPDH)). The relative gene expressions were determined by calculating $2^{-\Delta\Delta Ct}$.

2.5. Assessments of in vivo performance

The animal experiments were approved by the Guangdong University of Technology Ethics Committee. Thirty SD rats (body weight: 180–200 g) were anesthetized by intravenously injecting pentobarbital sodium (dosage: 20 mg per 1 kg body weight). A large critical-size bone defects with 6 mm in diameter were drilled in the skull. The rats were divided into three groups at random: calvarial defects without implantation, with Mg3 and Li2Mg2 bioceramic scaffolds. The incision was closed by suturing layer upon layer. At post-implantation weeks 6 and 12, the rats were sacrificed, and the scaffold-tissue constructs were harvested, and fixed with 10 vol.% formalin solution. A microcomputed tomography (μ-CT) system (NanoVoxel 30000D, Sanying Precision Instruments Co., Ltd., China) was utilized to evaluate the bone regeneration in the calvarial defects of rats. Decalcification of the samples were conducted by immersion in the 10% ethylene diamine tetraacetic acid solution for 4 weeks. The decalcified samples were embedded within the paraffin blocks. 5 μm thick slices were cut from the blocks with a microtome, and subsequently stained with hematoxylin and eosin (HE) solution. The blood vessels in the defect sites were

evaluated by immunohistochemical staining of platelet endothelial cell adhesion molecule-1 (CD31), which constitutively exists in the endothelial cells.

2.6. Statistical analysis

The differences between the experimental groups were analyzed by student's t-test. $P \leq 0.05$ was considered statistically significant.

Table S1. Primer sequences used for RT-PCR in the study.

Gene	Primer sequences
ALP	Forward: 5'-TGCCTACTTGTGTGGCGTGAA-3' Reverse: 5'-TCACCCGAGTGGTAGTCACAATG-3'
Col I	Forward: 5'-ATGCCGCGACCTCAAGATG-3' Reverse: 5'-TGAGGCACAGACGGCTGAGTA-3'
BSP	Forward: 5'-AGAACAATCCGTGCCACTCACTC-3' Reverse: 5'-AGTAGCGTGGCCGGTACTTAAAGA-3'
OCN	Forward: 5'-AGCAGCTTGGCCCAGACCTA-3' Reverse: 5'-TAGCGCCGGAGTCTGTTCACTAC-3'
VEGF	Forward: 5'-TGCGGATCAAACCTCACCA-3' Reverse:5'-CAGGGATTTTTCTTGTCTTGCT-3'
KDR	Forward: 5'-GTGATCGGAAATGACACTGGAG-3' Reverse: 5'-CATGTTGGTCACTAACAGAAGCA-3'
HIF-1α	Forward: 5'-CCATGTGACCATGAGGAAAT-3' Reverse: 5'-CGGCTAGTTAGGGTACACTT-3'
GAPDH	Forward: 5'-TGTGTCCGTCGTGGATCTGA-3' Reverse: 5'-TTGCTGTTGAAGTCGCAGGAG-3'

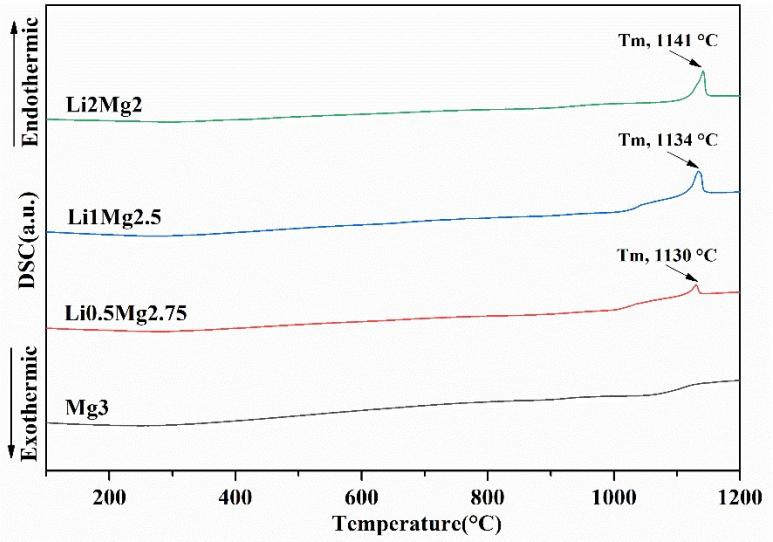

Fig. S1. DSC curves of synthesized Mg3, Li0.5Mg2.75, Li1Mg2.5 and Li2Mg2 powders.